Chiral-Induced Spin Selectivity Effect

R. Naaman*

Department of Chemical Physics, Weizmann Institute of Science, Rehovot, 76100, Israel

David H. Waldeck*

Department of Chemistry, University of Pittsburgh, Pittsburgh, Pennsylvania 15260, United States

ABSTRACT: The chiral-induced spin selectivity (CISS) effect was recently established experimentally and theoretically. Here, we review some of the new findings and discuss applications that can result from special properties of this effect, like the reduction of the elastic backscattering in electron transfer through chiral molecules. The CISS effect opens the possibility of using chiral molecules in spintronics applications and for providing a deeper understanding of spin-selective processes in biology.
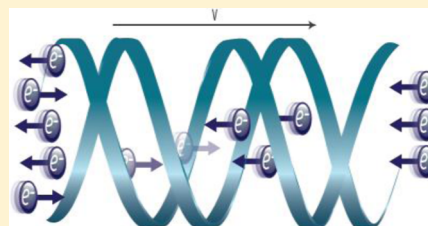
Before the development of quantum mechanics, scientific theories for the structure of matter and its properties were based on the concepts of mass and charge. As quantum mechanics was being formulated, however, it became evident that a new property of matter exists, the spin or intrinsic angular momentum of elementary particles. For the case of electrons, the spin is associated with two states, commonly referred to as spin "up" and spin "down"; in the absence of a magnetic field, these two states are degenerate. In the presence of magnetic interactions, this degeneracy is removed, and the spin states split; however, the energy gap between spin orientations is typically small as compared to the thermal energy, kT, at room temperature. Despite the fact that magnetic interactions are so much weaker than typical electrostatic interactions, the effect of spin on the structure and function of matter is very substantial because of its importance for the molecular (or atomic) wavefunction's symmetry. In addition, the spin of charged particles is associated with an intrinsic magnetic moment and is the essential feature underlying the magnetic properties of matter.

Spin is manifest in reactions of organic molecules[1−3] and in spectroscopy;[4] however, spin-selective electron transfer or transport is usually associated either with magnetic materials or with materials that have very large spin−orbit coupling (SOC). For example, the giant magnetoresistance (GMR) effect, which is important to technologies used in magnetic memories, results from spin-selective transport through two ferromagnetic layers separated by a thin nonmagnetic layer.[5,6] Also, it has been suggested that spin-selective transport can be obtained in solid-state devices based on GaAs, which has a large SOC.[7,8] In this case, the material is required to lack inversion symmetry, and the selectivity arises from the coupling of the linear momentum with the spin. The SOC that acts on the propagating electrons is referred to as Dresselhaus[9] or Rashba,[10] depending on whether they originate from bulk or structure inversion asymmetry, respectively.

The idea of combining spin properties with electronics is now under intensive study in what is called "spintronics".[11−13] The spin has a number of important attributes, which make it highly desirable for transferring and manipulating information. One attribute is that the energy required for switching the orientation from up to down, or vice versa, is very small; thus, the energy required to move, or change, spin information can be small. In addition, the spin is weakly coupled to bath modes so that the "coherence" of spin states can be preserved for a relatively extended period of time.[14] Therefore, superposition states of spin systems are being explored for quantum information transfer and quantum computation.[15]

Despite the success of inorganic-material-based spin devices, intensive research is focused also on "organic spintronics", where organic molecules are used within spin-specific devices.[16,17] Most commonly, the organic material is used as a medium that transfers the spin without altering its magnitude or its direction. Magnetic organic molecules, which are being considered as electronic device analogues, are not yet at the stage that they can be applied as spin filters at room temperature.[18,19] Recent work on spin selectivity in chiral molecules and molecules with chiral secondary structure promises to change this picture, however.

Chiral molecules are those that have identical composition, connectivity, and conformation but have a nonsuperimposable mirror image, so that they can exist as two different molecules or distinguishable enantiomers.[20] Because many biomolecules are chiral and many biochemical reactions involve chiral molecules, much effort has been placed on understanding enantioselectivity in chemical transformations[21−23] and the properties of chiral molecules.[24] Chiral molecules break parity symmetry; however, they retain time-reversal symmetry, and it

is necessary to have a charge flowing through them in order to break time-reversal symmetry and thus meet the symmetry requirements for generating a magnetic field along the charge's velocity direction.[25]

> Recent electron transmission experiments have shown unequivocally that ordered films of chiral organic molecules on surfaces can act as electron spin filters at room temperature, an effect that we term chiral-induced spin selectivity (CISS).

Recent electron transmission experiments have shown unequivocally that ordered films of chiral organic molecules on surfaces can act as electron spin filters at room temperature, an effect that we term chiral-induced spin selectivity (CISS).[26] The spin polarization or spin selectivity (S) is defined as

$$S = \frac{I_+ - I_-}{I_+ + I_-} \tag{1}$$

in which I_+ and I_- are the intensities of the signals corresponding to the spin oriented parallel and antiparallel to the electrons' velocity, respectively. Although results pointing to this effect have been available for more than a decade,[27−29] the lack of a theoretical explanation for its origin and the availability of only indirect evidence for the spin polarization has hampered its development. In addition to these limitations, early work on gas-phase molecules displayed a very small spin selectivity in electron scattering, on the order of 10^{-4}, which discouraged investigations into this phenomenon.[30,31] Recent developments, both theoretical and experimental, have changed this situation, and the CISS effect, with a spin selectivity 10 000 times larger than that found in gas-phase molecules, has a much stronger footing.

In the following, we provide first a discussion of theoretical developments concerning the origin of spin-selective transport through chiral molecules; then, we discuss experimental observations that have led to the discovery of the CISS effect, and we end with a discussion of the possible implications and future applications of CISS.

■ THEORETICAL BACKGROUND

While a qualitative understanding for the origin of the CISS effect has been available, only recently has important progress been made in providing quantitatively accurate calculations of spin polarization yields. In CISS, the molecules' chirality is a requirement for spin selectivity to occur. As an electron moves along a chiral molecule, it experiences the electrostatic potential of the molecule, which is also chiral. In the electron's rest frame, the current generates a magnetic field $\vec{B}$

$$\vec{B} = \frac{\vec{v}}{c^2} \times \vec{E}_{chiral} \tag{2}$$

in which $\vec{v}$ is the velocity of the moving electron, c is the speed of light, and $\vec{E}_{chiral}$ is the electric field acting on the electron while it moves through the chiral molecule (see Figure 1a). Because the electron has a magnetic dipole associated with its spin, the two spin states that are degenerate when no magnetic field exists are now split. Note that because of the three-dimensional nature of the chiral molecules, a component of the magnetic field lies parallel (or antiparallel) to the electron's velocity direction.

What is $\vec{E}_{chiral}$? The electric field acting on the moving electron must arise from the electrons and nuclei that comprise the chiral molecule. For an electron with a speed of 0.2% of the speed of light, an electric field of 4.5×10^{11} V/m would generate a magnetic field of 3 T. This electric field is comparable to that experienced by an electron in the ground
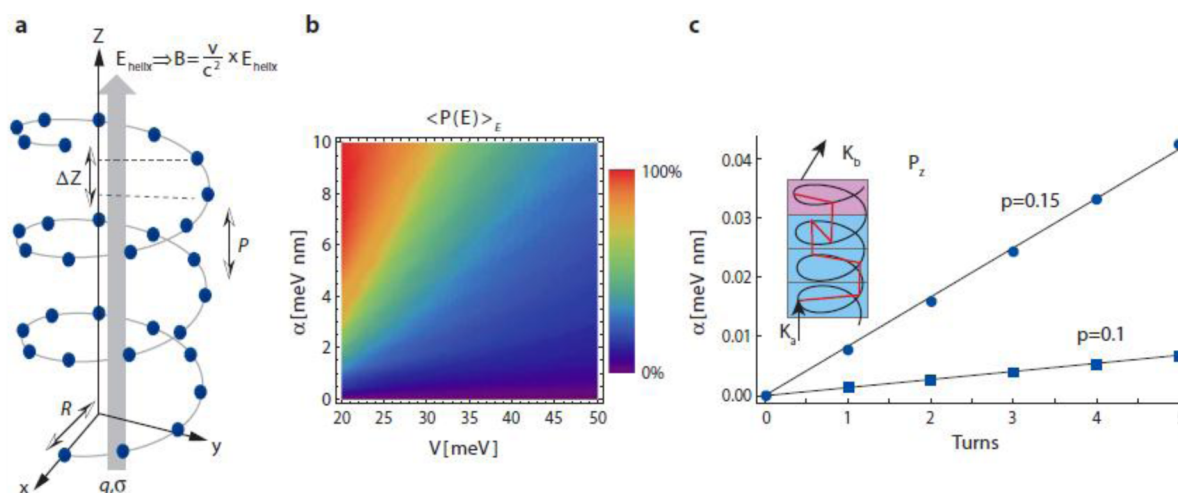
Figure 1. (a) The essential physical picture of a charge q in spin state σ moving along the axis of a helical charge distribution (blue dots). The parameters are the helix pitch, p, the radius, R, and the spacing of the Δz component of the position vector of the charges distributed along it. The helical field $\vec{E}_{helix}$ induces a magnetic field $\vec{B}$ in the rest frame of the charge and hence influences its spin state. (b) A two-dimensional plot of the energy-averaged spin polarization, $\langle P(E) \rangle_E$, as a function of the electronic coupling V and the SOC parameter, α. Spin polarization is stronger for small V and larger SOC. (a,b) Reprinted from ref 40 with permission. (c) The longitudinal polarization plotted as a function of the number of turns in the helix for $p < R = 1.88$ au and the wavevector $K = 1$ au. The polarization grows linearly with helix length; however the slope of the dependence depends on the pitch. The inset depicts the incoherent scattering from separate slabs of one turn in thickness. The figure is reprinted with permission from ref 38.

state of a hydrogen atom. For some of the effects described below, the effective magnetic field must be 10−100 times larger, implying that the electric field must be 10−100 times larger; thus, while the field will have contributions from valence electrons, it must also involve inner-shell electrons. This aspect has been pointed out for the case of electron scattering in semiconductor devices.[32]

The term in the Hamiltonian for the SOC[33] is given by

$$H_{SO} = \lambda \vec{\sigma} \cdot (\vec{p} \times \vec{E}_{chiral}) \tag{3}$$

in which $\lambda = (e\hbar)/(4m^2c^2)$, $\vec{p}$ is the electron momentum, m is the electron's mass, and $\vec{\sigma}$ is a vector whose components are the Pauli matrices σ_x, σ_y, and σ_z. For convenience, we express H_{SO} as $H_{SO} = (1/h)\vec{\sigma} \cdot (\vec{p} \times \vec{\alpha})$ in which $\vec{\alpha} = \hbar\lambda\vec{E}_{chiral}$. Equation 3 arises directly from the Pauli equation, and it indicates a coupling between the linear momentum of the electron and its spin. If we recast eq 3 in the form of that for the energy of an electron spin in a magnetic field $\vec{B}$, namely $-\mu_B g\vec{\sigma} \cdot \vec{B}$, we can find an effective magnetic field, $\vec{B}_{eff} = -(\vec{v} \times \vec{E}_{chiral})/(2c)^2$. This magnetic field differs from that in eq 2 by a factor of 2 because of a correction for relativistic effects.[34]

Recently, three different theoretical groups have developed models to explain the CISS effect in helix-shaped molecules, in general, and in double-strand DNA, in particular. Although these models differ in some important ways, they also have important commonalities. Each of these models is based on calculating the spin−orbit interaction of an electron spin that is moving through a helical potential by way of the Rashba SOC term (eq 3),[10] and each demonstrates that the chirality is essential for obtaining spin polarization. In addition, these workers use a SOC value that is significantly larger than the value found for low Z atoms, which are typical of organic molecules, and rationalize this value in terms of the molecule's secondary structure. This feature of a larger SOC has been suggested for carbon nanotubes,[35−37] and it was calculated for the CISS case by Medina et al.[38] These theoretical treatments and recent experimental measurements for carbon nanotubes[39] give a value of a few meV for the SOC magnitude.

In the first work, Gutierrez et al.[40] constructed a simplified model that places point charges along a helical path with a radius R and a pitch p, rather than attempting to construct a realistic model for a DNA molecule or α-helical peptide (Figure 1a). They used a tight binding model for the electronic structure of the helix and computed the transmission of distinct electron spin states by way of the Landauer formulation,[41] in the approximation that the electrons have $p_z \neq 0$ and $p_x = 0 = p_y$. Through rough estimates for the electron coupling V between sites on the helix and the SOC coupling parameter α, they defined a reasonable parameter range in which they compute the spin polarization. Their model displays the spin filtering effect and indicates that it is most pronounced for electron energies near the edges of the tight binding band. Figure 1b (adapted from Figure 4 of ref 40) shows the dependence of the energy-averaged spin polarization on V and α for a helix with a radius of 1 nm and a pitch length of 3.2 nm, parameters appropriate for DNA.

As expected, their calculations show that large SOC (larger α) lead to more spin polarization; however, the spin polarization is strongly decreased for higher electronic couplings. They propose that this reduction in the spin polarization results because the characteristic time, $\hbar/V$, is decreased for larger V, and this decreases the interaction time between the electron and the chiral field. Although the

treatment is schematic and does not simulate exactly the molecules studied, it results in a large spin polarization effect, and the polarization arises from the spin interacting with an "effective magnetic field" that is generated by the electron motion through a helical electrostatic potential. They conclude that the spin polarization effect is relatively large because of the resonance states that result in a relatively low mobility of the electron in the potential.[40]

Guo and Sun[42] have presented a model that treats the double helix of ds-DNA in an explicit manner, and they computed the spin-dependent conductance through a metal−DNA−metal structure. They used a "two leg ladder" model for the DNA and included dephasing of the ladder states. The charge transport is assumed to proceed along each strand, and it is described through a tight binding picture. They show that both the SOC and the helical nature of the DNA duplex are required for spin polarization. They also examined the relationship between the DNA's length and the dephasing strength to reveal that an optimal/critical length exists for which the spin polarization reaches a maximum. For short chains, they found that the polarization increases with the dephasing strength, but as the length becomes long enough that significant dephasing of the spin amplitude occurs, then the spin polarization declines. The value of the critical length decreases as an inverse function of the dephasing strength.

A third theoretical description has been given by Medina et al.,[38] in which they used scattering calculations to obtain the spin polarization of electrons moving through chiral molecules with energies above the vacuum level. Following an earlier study,[43] they conducted scattering calculations, and their treatment used a simplified model for the molecule that is comprised of six carbons atoms, which act as the electron-scattering centers, arranged on a helix so that it completes one full turn. Because the Rashba SOC term gives rise to the spin selectivity, their calculations required multiple scatterings for the generation of a longitudinal spin polarization, that is, spin polarized parallel or antiparallel to the propagation direction of the electrons. Their investigation reveals that the spin selection involves an interference between the spin−orbit scattering amplitudes and those from the pure electrostatic terms and that well-defined energy ranges (or energy windows) of high spin polarization occur. For this model system of six carbon sites in a single turn, they found a polarization of about 1%. While this value is significant in magnitude, it is much smaller than that found in experiments for DNA and polypeptide assemblies (vide infra); the authors suggest that when the density of atoms is higher, as is the case in DNA, the spin polarization will be higher. They illustrate this effect by constructing an incoherent superposition that shows a linear increase of the polarization with the number of helix turns and has a slope that depends on the helix's pitch (see Figure 1c and Figure 4 of ref 38).

While these three studies differ in important ways, they possess very similar physical phenomenology. In particular, they show that a chiral potential causes a significant coupling between a particle's linear momentum and its spin, even for the situation in which the atomic SOC is small (atoms with low atomic number). These studies point to two important factors that affect the CISS. First, they reveal that the value of the SOC for the chiral molecule must be larger than the atomic SOC by 1−2 orders of magnitude. While such values have been reported for carbon nanotubes, we do not know of such measurements for DNA or polypeptides. Second, they predict particular energy ranges, or resonances, in which the spin

polarization will be high, a feature that should be explored experimentally. The energy windows arise from different effects however, and combining such studies with the polarization's dependence on the number of turns and the helical pitch may be able to distinguish between the models.

> A chiral potential causes a significant coupling between a particle's linear momentum and its spin, even for the situation in which the atomic SOC is small (atoms with low atomic number).

The coupling of the electron's linear momentum and its spin has an important implication for the efficiency of charge transport and the sense of the molecular helix. The freely propagating electron has four states associated with its motion, which we denote by $|+,+\rangle$, $|-,-\rangle$, $|+,-\rangle$, and $|-,+\rangle$, in which the first variable relates to the direction of motion and the second to the direction of the spin (see Figure 2). For an electron
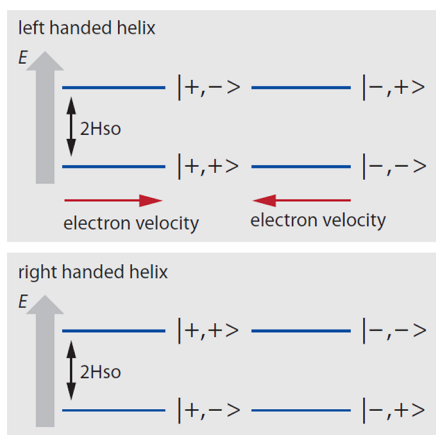
Figure 2. An energy scheme is shown for the momentum-spin states, |momentum,spin⟩, of an electron moving within a chiral potential. The spin alignment flips with the handedness of the helix.

moving in the positive (+) direction through a left-handed helix, its up spin (+) is stabilized relative to its down spin (−); that is, $|+,+\rangle$ is the ground state, and the state $|+,-\rangle$ lies at higher energy with a gap corresponding to twice H_{SO} (see eq 3). Thus, one state is stabilized by the spin−orbit energy, and the other is destabilized by the same energy, so that the difference between the states is twice the value of H_{SO}. Furthermore, the $|+,+\rangle$ state is degenerate with the state $|-,-\rangle$, which corresponds to the electron moving in the opposite direction with the opposite spin. The state $|+,-\rangle$ lying at higher energy is degenerate with the state $|-,+\rangle$. In the case of the opposite molecular handedness, the states $|+,-\rangle$ and $|-,+\rangle$ will be the degenerate ground states, and $|+,+\rangle$ and $|-,-\rangle$ will be the higher-lying states (see Figure 2). Returning to the first case, for an electron to be elastically backscattered within a helical molecule, it has to change its state from $|+,+\rangle$ to $|-,-\rangle$, which requires a change in spin as well as momentum, thereby making it unlikely.

Because the experiments performed so far have been conducted at room temperature, one has to consider the thermal distribution of electron energies when discussing the

possibility for backscattering. For an electron to be back-scattered and retain its original spin orientation, it must acquire an energy exceeding two times H_{SO}, so as to populate one of the higher-lying momentum-spin states (in the specific example given above, it corresponds to populating the state $|-,+\rangle$), and the fraction of the population that has energy exceeding the energy of the $|-,+\rangle$ state is given by

$$P_{bs} = \exp\left(-\frac{2H_{SO}}{kT}\right)$$

(4)

For $H_{SO} = 20$ meV, which is typical in the theoretical calculations described above, about 20% of the population (at room temperature) will have enough energy to be back-scattered with no spin-flip, namely, the backscattering cross section will be reduced by a factor of about 5. As discussed below, experiments indicate that the value of H_{SO} in DNA oligomers is on the order of 0.5 eV, making elastic backscattering that does not include spin-flipping highly improbable.

It is important to note that some studies identified a dependence of the spin polarization's sign on the direction of the adsorbed molecule's dipole moment, and this feature has not been explicitly treated in the calculations described above. Recently, a new model of the spin order in self-assembled monolayers (SAMs) of chiral molecules has been developed[44] to explain these experimental results. This model is based on the coupling between linear momentum and spin for an electron moving on a curved trajectory, and it points to a cooperative spin effect that arises in SAMs of chiral molecules and will be discussed with the relevant experiments, vide infra.

■ EXPERIMENTAL RESULTS

Photoemission Studies. The first indications for the CISS effect were obtained from low-energy photoelectron transmission (LEPET) spectroscopy studies of Langmuir−Blodgett films comprised of chiral molecules.[27,45] In this work, Langmuir−Blodgett films of amino acids were deposited on a polycrystalline gold substrate.[27] The LB films consisted of either L- or D-stearoyl lysine $[(CH_3(CH_2)_{16}C(O)NH-(CH_2)_4CH(NH_3^+)-CO_2^-]$, and FTIR studies demonstrated that the film's order and geometry were independent of the molecular enantiomer. In the LEPET experiment (see schematic diagram, Figure 3a), circularly polarized light was used to eject spin-polarized photoelectrons from the underlying Au substrate,[46−49] and the quantum yield and kinetic energy distribution of the photoelectrons were measured for different molecular assemblies. It was found that the quantum yield of photoelectrons depended on the relative polarization of the light and the chirality of the molecules in the LB film. For example, right-handed circularly polarized light showed a higher quantum yield of photoelectrons through an L-stearoyl lysine assembly than that through an R-stearoyl lysine assembly, even though the film thickness and order were the same. Correspondingly, these experiments showed that the quantum yield of photoelectrons through an L-stearoyl lysine assembly was highest for right-circularly polarized light, intermediate for linearly polarized light (no net spin polarization from the Au), and smallest for left-circularly polarized light. The polarization of the photo-emitted electrons from the Au is positive (spin vector parallel to the electron's velocity) when the photon is right-circularly polarized, and the polarization of the photoelectron distribution ranged from 5%[50] at kinetic energies near 0 eV to about 15% at
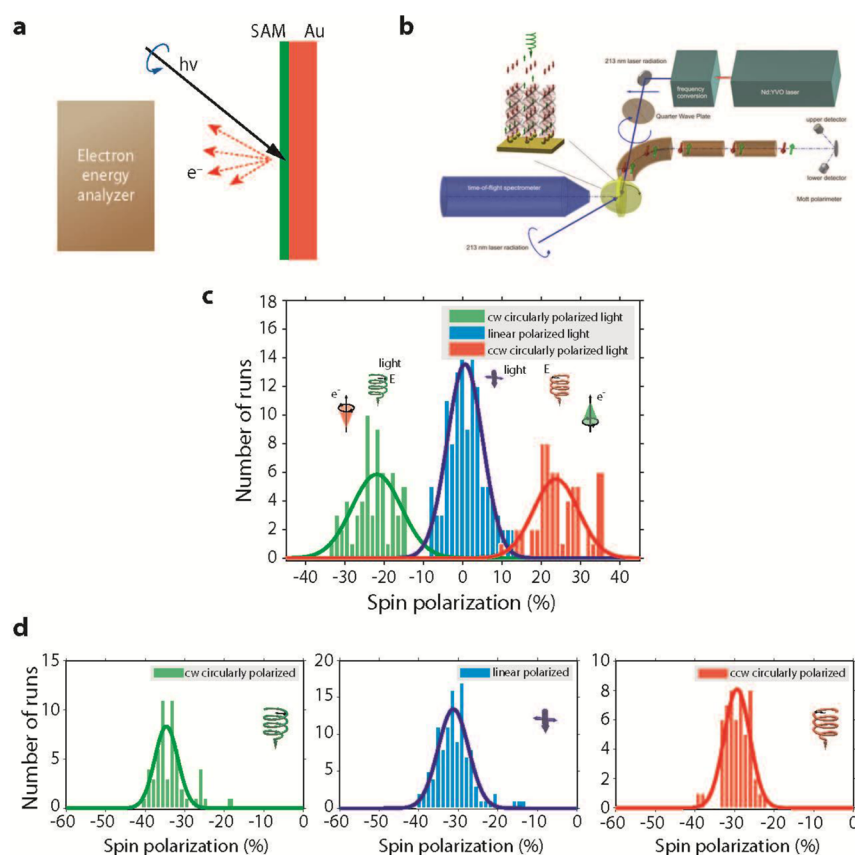
Figure 3. (a) A scheme for the LEPET photoemission setup for measuring electron energy distributions through chiral monolayers, without resolving the spin of the transmitted electron. (b) The scheme of the experimental setup for measuring the spin polarization of the photoelectrons. The plot in panel (c) shows the polarized electron distributions measured for electrons ejected from bare Au(111) with clockwise circularly polarized light (cw: green), counterclockwise circularly polarized light (ccw: red), and linearly polarized light (blue). The mean longitudinal spin polarizations are −22, +22, and 0%, respectively. (d) The longitudinal spin polarization distributions for electrons transmitted through 50-bp dsDNA/Au(111). In this case, the mean spin polarizations were nearly independent of the incident light polarization: −35 for cw circularly polarized (green), −31% for linearly polarized (blue), and −29% for ccw circularly polarized (red). (b−d) Reprinted with permission from ref 26.

2 eV.[51] Recent studies that were performed on single-crystal Au (111) surfaces coated with DNA molecules found up to 20% spin polarization.[26]

These experiments indicate that the LEPET signal is correlated with the spin polarization, indicating spin selectivity in the photoelectrons' transmission through the chiral monolayers. The effect amounts to about a 5−7% difference in the transmission efficiency between the two spins for a given handedness of the monolayer. This value is already larger by 3 orders of magnitude than that observed in electron scattering from gas-phase chiral molecules.[51] However, if one considers that the spin polarization of photoelectrons that arises from the Au substrate is only about 15−20%,[46−49] then this 5−7% difference amounts to a 30−50% selectivity in the transmission.

The LEPET experiments of stearoyl lysines demonstrated that the scattering of the photoelectrons from the adsorbed molecules depends on the light's helicity and the molecule's chirality. By studying multilayer films (films up to five monolayers thick were studied), the chirality of the molecules could be changed between the layers, and it was found that changing the molecules' chirality between layers decreased the quantum yield of photoelectrons and shifted the kinetic energy distribution to lower average energy. These observations can be understood by considering that the electron−molecule scattering depends on the electron spin and the chirality of the scattering center. In addition to changing the chirality of the

different monolayers in a multilayer assembly, it is also possible to mix the two enantiomers within a monolayer. These experiments showed that the asymmetry in the photoelectron yield was no longer evident for mixtures that were 99% of one handedness and only 1% of the other. This latter experiment indicates that the transmission of photoelectrons through the organic films is coherent and that the electron wavepacket interacts with many molecules as it propagates.

Following this first study, several other LEPET studies on SAMs of chiral molecules were conducted,[28,29,52] including SAMs of polyalanine[28] and SAMs of double-stranded DNA[29] In ref 52, the CISS effect was observed when the photoelectrons had kinetic energy of tens of eV. All of these studies confirmed the dependence of the electron transmission yield on the chirality of the molecules and the handedness of the light that was used to eject photoelectrons from the underlying gold substrate. In the study of α-helix polyalanine monolayers, it was possible to confirm the dependence of the spin selectivity on the handedness of the molecules; however, a dependence on the direction of the molecules' dipole moment was also observed. This dependence on the dipole moment was not discussed in the theoretical studies described above; however, it has been discussed and explained in another qualitative theory.[44] This theory assumes that the photoemission is observed from hybrid states, in which the molecular and the substrate states are mixed to form spin states with properties

that depend on the handedness of the molecules and the direction of their dipole moments. In the study of DNA, it was established that the extent of spin polarization depends on the helix structure of the double-stranded DNA, while for the single-strand DNA no significant polarization could be detected.

While these experiments reveal a clear dependence of the photoelectron yield on the light's polarization and the chirality of the molecular films, the relationship of these effects to the spin polarization of the photoelectrons was only inferred. A recent experiment by Göhler et al.[26] has removed this weakness and demonstrated convincingly that molecular assemblies of chiral molecules act as efficient spin filters for photoelectrons. Göhler et al. performed a LEPET-type experiment in which they measured the spin of the photoelectrons with a Mott detector after they were transmitted through a SAM of double-stranded DNA (Figure 3b). The data in Figure 3c show that the spin polarization of the photoelectrons from a bare Au(111) surface can be manipulated by choice of the light polarization, ranging from −22% for right-handed polarized light to 0% for linearly polarized light and +22% for left-handed polarized light. When a SAM composed of DNA molecules is adsorbed on the metal surface, however, the spin polarization of the photo-electrons does not change significantly with the light polar-ization, only ranging from −35% to −29% (see Figure 3d). Thus, the DNA molecules act as a selection filter for the electrons' spin polarization. Furthermore, they showed that the amount of spin polarization increases monotonically with the length of the DNA duplex, reaching a value of about 60% for SAMs composed of duplex DNA with 78 base pairs. This latter study demonstrates that the spin polarization (CISS) is not a result of the gold−SAM interface but is caused by the properties of the chiral molecules.

In agreement with earlier studies,[29] they showed that the spin polarization of photoelectrons, which are transmitted through a SAM composed of double-stranded DNA, is much larger than that found for SAMs composed of single-stranded DNA, by an order of magnitude. Furthermore, they observed that the spin polarization in the two cases has the opposite sign. Although the electronic asymmetry has a simple geometrical interpreta-tion for helical secondary structure, no such interpretation is possible for molecules that simply contain a chiral center. Although the chirality of an atomic center is defined in terms of the spatial order of the atoms bonded to it, their relationship to the electronic nature of the center has no simple geometrical interpretation.

Electron Transfer and Transport. In photoemission experi-ments, the photoelectrons have an energy above the vacuum level as they transit through the organic layer and then to the detector. The importance of this fact for the spin filtering effect has been evaluated by examining the CISS effect for electron energies in the tunneling regime, using photoelectrochemistry[53] and single-molecule conductance[54] experiments. The impor-tance of CISS in electron tunneling was examined in a photoelectrochemical cell for which a porphyrin chromophore was adsorbed to a gold electrode through a chiral bridging unit. In this experiment, the SAM was coated onto a gold film, which served as the working electrode, and the dependence of the photocurrent on the polarization of the incident light and the chirality of the molecular bridging unit was examined. By using a methylviologen redox acceptor, the cathodic photocurrent was made highly stable, so that extensive photocurrent and action spectra could be collected. Upon excitation with

circularly polarized light, the photocurrent displayed an asymmetry (different magnitude of photocurrent for right versus left polarization) that changed with the molecular chirality (left- or right-handedness of the scaffold); see Figure 4.
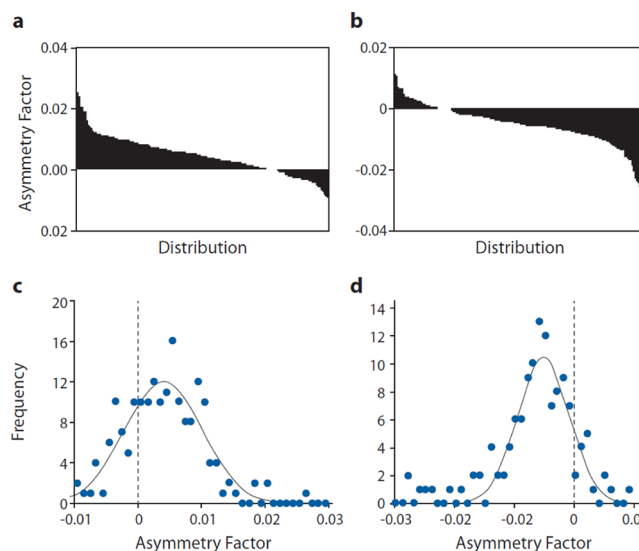

Figure 4. Distributions of asymmetry factors and statistical analysis of the helicities. (a,b) The distributions of the asymmetry factors in a descending sort for **R1** and **S1** scaffold porphyrin electrodes, respectively; (c,d) The histograms of the number of observations versus the observed ranges of asymmetry factors, corresponding to panels (a) and (b), respectively. Reprinted with permission from ref 53.

The observed changes in the photocurrent with light polarization were small, so that extensive averaging over time for a given electrode and over multiple electrodes had to be performed in order to quantify the effect. The average asymmetry factor obtained for a right-handed monolayer was 0.004 ± 0.002, and that for a left-handed monolayer was −0.005 ± 0.001, in which the error represents confidence limits of 95%. Figure 4 plots the distribution of asymmetry factors for the two different chiralities of the SAM-coated electrodes.

The relatively small CISS effect that is observed in this experiment could result for several reasons. Even if one assumes that the spin selectivity of the chiral bridging unit is 100%, asymmetry in the photocurrent could be decreased if the orbital angular momentum of the optically prepared excited state is not converted efficiently to a specific spin state. In part, this conversion efficiency depends on the SOC in the chromophore, which could be small for the free porphyrin used in this system. Even if the excitation results in a well-defined spin orientation, it is also necessary that the spin's orientation be parallel or antiparallel to the axis of the chiral system for efficient selectivity. Thus, any misalignment will cause a mixture of the two spin orientations and hence a reduction in the selectivity.

More recently, CISS in the tunneling regime was demonstrated by measuring the single-molecule conductance of double-stranded DNA molecules for spin-polarized electrons injected either parallel or antiparallel to the helical axis; Figure 5a shows a schematic of the experimental design.[54] In this study, single-stranded, thiolated DNA molecules were adsorbed onto a Ni substrate, and then, the assembly was exposed to a solution containing the complementary DNA strand, which was bound to a gold nanoparticle on one end, so that a Ni−
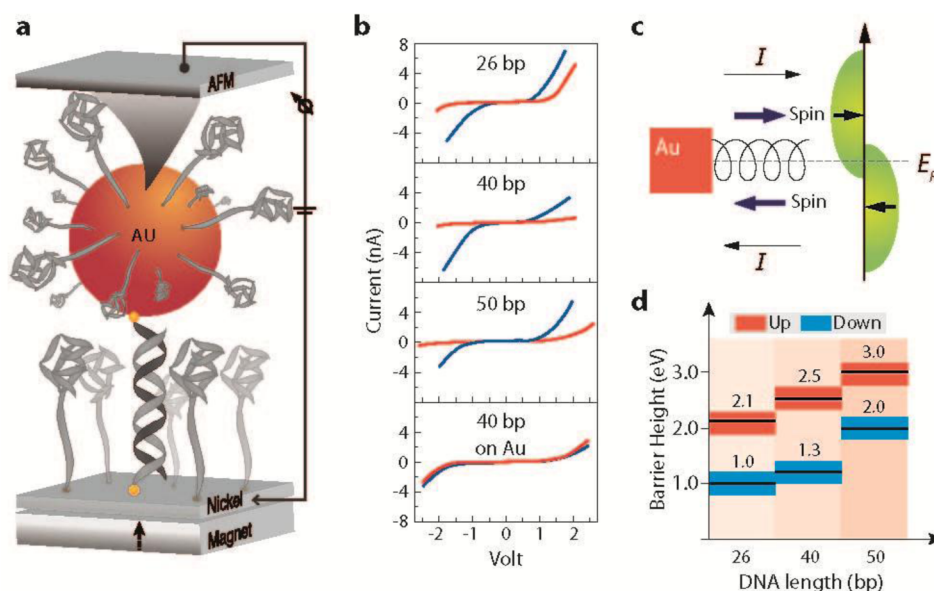
Figure 5. (a) The experimental scheme for measuring the conductance of a nanoparticle−dsDNA−nickel molecular junction. The permanent magnet, underneath of the nickel substrate (bottom electrode), splits the sub-bands of the Ni (see Figure 4c). The current is measured between the nickel substrate and the tip of the AFM, which is placed in contact with the gold nanoparticle (top electrode). (b) The average current obtained for the three oligomers studied when the magnetic field is pointing up (red) or down (blue). For control, the bottom panel shows the signal obtained with a gold substrate when no specific spin is injected. (c) A scheme of the density of states in magnetized nickel. When electrons flow from the Ni, their spin is the majority spin, while electrons flowing from the gold nanoparticle to the Ni must have the minority spin in order to be injected into the Ni. (d) The effective barrier extrapolated from the dI/dV curves in panel (c) are shown, when the magnet is pointing down (blue) or up (red). The widths of the lines reflect the uncertainty in determining the effective band gap, which is ± 0.2 V. (a,b,d) Reprinted with permission from ref 54.

molecule−Au junction was formed upon hybridization. A conductive AFM tip, operating in contact mode, was used for measuring the $I−V$ curves, and this was done for different magnetizations of the Ni substrate. Magnetization of the Ni substrate breaks the degeneracy of the Ni's valence electrons and creates two overlapping conduction bands, one corresponding to electrons whose spins are aligned with the magnetic field and the other corresponding to spins aligned against the magnetic field.

A simple inspection of the average $I−V$ curves shown in Figure 5b demonstrates clearly that the molecule's conductance depends on the magnetic field direction and on the length of the DNA molecules. In particular, note that when the magnetic field is oriented up that the diode-like shape of the $I−V$ curve indicates a lower effective barrier than that for the case when the magnetic field is oriented down. Note also that the $I−V$ curves are symmetric, that is, the same spin alignment of the electrons is favored both for positive and negative voltage biases. The relation between spin conduction and the magnetization of the Ni is schematically described in Figure 5c. When electrons are ejected out of the magnetized Ni, they are mostly majority electrons (from the more stable sub-band). If their spin orientation is consistent with the favored spin orientation for transmission through the chiral molecule, then the current for this magnetic field direction will be higher than the current measured under the situation where the Ni is magnetized in the opposite direction and the electrons have the opposite spin orientation, which is disfavored by the DNA helix. When electrons are conducted in the opposite direction (e.g., negative current rather than positive current), the favored spin orientation is aligned in the opposite direction. This spin orientation coincides with the minority electron sub-band in the Ni, which has a high density of states above the Fermi energy, and therefore, it favors electron injection into the Ni.

Hence the $I−V$ curve is expected to be symmetric, in agreement with the experimental observation.

Figure 5d presents the effective barriers that were obtained from the $I−V$ curves of the double-stranded DNA oligomers for spins aligned both parallel and antiparallel to the current direction. This graph shows that the effective barrier increases with the length of the DNA duplexes but that the difference between the barriers for the two spins is constant for all lengths and is about 1 eV. Because the difference in the effective barrier energies arises from the two different spin orientations, one can use eq 3 to extract the SOC energy (H_{SO}). Taking the energy difference between the two spin orientations to be $2H_{SO}$ and the difference in effective barrier to be 1 eV, we obtain $H_{SO} \approx$ 0.5 eV. This energy gives an α on the order of 50 meV−nm as compared to the 1−6 meV−nm values used in the calculations. Thus, the experiment indicates that the SOC term for charge moving through a helical macromolecule is even larger than that used in the calculations.

Implications and Applications. CISS in Biology. A large fraction of biologically important chemical transformations involve redox chemistry with chiral molecules or occur in environments containing chiral molecules. Because of the coupling between the linear momentum and the spin, the CISS effect may play an important role in some electron-transfer and charge recombination reactions. The coupling of the charge's spin orientation to its velocity implies that electron transfer through a chiral bridge will be biased in one direction because elastic backscattering (coherent charge recombination) must include a spin-flip process, which is much less probable. Thus, the probability of charge separation would be inherently different from charge recombination on time scales shorter than the spin state's decoherence time. Thus, one expects that these electron-transfer processes may be affected by the electron spin, and/or that magnetic fields could perturb biochemical

processes. While conventional wisdom generally considers magnetic field perturbations on biological processes to be minor, or simply a curiosity, recent considerations indicate that re-evaluation is needed.[55,56]

Without reliable elementary models for the interactions, it is difficult to design, reproduce, and interpret experiments that probe these processes. In addition to biochemical processes,[57] growing interest exists in understanding how weak magnetic fields affect navigation by birds and fish. The possibility of quantum evolution of a spatially separated pair of electron spins was discussed recently for several biosystems[58,59] and especially in relation to bird and fish navigation.[60] If indeed CISS takes place in biology, it may help to explain what interactions (at the level of electrons, atoms, and molecules) give rise to magnetic field effects on living systems. CISS-related studies may shed new light on these fascinating subjects.

CISS in Spintronics. The CISS effect provides a way to create spin-polarized electrons without use of a magnet and opens new possibilities for spintronics, in which most devices are currently constructed from magnetic materials. The ability to use a single molecular layer as a spin filter, instead of the common inorganic spin filter in which one layer is a permanent magnet, promises greater energy efficiency and reduction in device size. The availability of an efficient source of spin-polarized electrons makes it possible to magnetize ferromagnets by spin torque transfer.[61,62] Such devices are straightforward to produce, and because of the high spin selectivity observed in some of the chiral molecules, much less current may be required for switching these devices.

One manifestation of a memory device may be envisioned as containing a ferromagnetic nano-object that is placed between two electrodes (referred to as L and R) and connected to them by chiral molecules having all of the same handedness. Because the preferred orientation of the spin transmitted through the chiral molecules depends on the direction of charge flow, let us consider that charge is flowing from L to R through the chiral molecules and the nano-object. The preferred spin will be transmitted and can be used to induce magnetization in the nano-object by spin torque transfer, under high operating currents. After magnetization of the nano-object, a small current flowing from L to R will have a high resistance, while a small current flowing in the opposite direction will have a lower resistance because its spin will correspond to the minority spin in the nano-object. Of course, magnetizing the nano-object by large current flowing from R to L will have the opposite effect. Hence, a magnetic memory device can be constructed with no need for a permanent magnet.

> The chiral-induced spin selectivity (CISS) effect opens the possibility of using chiral molecules in spintronics applications and for providing a deeper understanding of spin-selective processes in biology.

While CISS offers clear advantages, it will pose new challenges also. Among them are the challenges of finding chiral molecules that are stable enough while exposed to current and of combining organic and inorganic substances without introducing high barriers for conduction.

■ AUTHOR INFORMATION

Notes

The authors declare no competing financial interest.

Biographies

Ron Naaman completed his B.Sc. in Chemistry at the Ben Gurion University, Beer-Sheva, Israel, and his Ph.D. at the Weizmann Institute in Israel. He then moved for a postdoctoral fellowship to Stanford, California, for 2 years and then spent 1 year at the Chemistry Department at Harvard. In 1980, he returned to Israel and became a faculty member at the Weizmann Institute. His work is focused on new electronic properties that emerge from the formation of supramolecular structures. He studies the effect of formation of clusters and van der Waals complexes on the reactivity of molecules. This work was followed by studies of reactive properties and electronic properties of SAMs. In parallel, his research group explores the transfer of information through supramolecular systems and produces self-assembled electrical devices. Recently, he studied the spin-selective transfer properties of chiral molecules.

David H. Waldeck completed his B.Sc. in Chemistry at the University of Cincinnati, Cincinnati, OH, and his Ph.D. at the University of Chicago. He then moved to the University of California, Berkeley as an IBM Postdoctoral Fellow for 2 years. In 1985, he joined the chemistry faculty at the University of Pittsburgh. His research program uses methods of spectroscopy, electrochemistry, and microscopy to investigate primary processes in the condensed phase, which includes liquids, solids, and liquid/solid interfaces. Current themes of his research are the fundamental understanding of electron-transfer reactions, electron transport in supramolecular structures, and nanophotonics

■ ACKNOWLEDGMENTS

■ REFERENCES

(1) See, for example: Turro, N. J.; Khudyakov, I. V. Single-Phase Primary Electron Spin Polarization Transfer in Spin-Trapping Reactions. *Chem. Phys. Lett.* **1992**, *193*, 546−552.

(2) See, for example: Okazaki, M.; Toriyama, K. Control of a Chemical Reaction by Spin Manipulation of the Transient Radical Pair As Demonstrated for Isotope Enrichment. *J. Phys. Chem.* **1995**, *99*, 489−491.

(3) Rodgers, C. T. Magnetic Field Effects in Chemical Systems. *Pure Appl. Chem.* **2009**, *81*, 19−42.

(4) See, for example: Lund, A., Shiotani, M., Shimada, S. *Principles and Applications of ESR Spectroscopy*; Springer Verlag: Berlin, Germany, 2011.

(5) Baibich, M. N.; Broto, J. M.; Fert, A.; Nguyen Van Dau, F.; Petroff, F.; Etienne, P.; Creuzet, G.; Friederich, A.; Chazelas, J. Giant Magnetoresistance of (001)Fe/(001)Cr Magnetic Superlattices. *Phys. Rev. Lett.* **1988**, *61*, 2472−2475.

(6) Binasch, G.; Grünberg, P.; Saurenbach, F.; Zinn, W. Enhanced Magnetoresistance in Layered Magnetic Structures with Antiferromagnetic Interlayer Exchange. *Phys. Rev. B* **1989**, *39*, 4828−4830.

(7) Datta, B.; Das, S. Electronic Analog of the Electro-optic Modulator. *Appl. Phys. Lett.* **1990**, *56*, 665−667.

(8) Lu, J. P.; Yau, J. B.; Shukla, S. P.; Shayegan, M. Tunable Spin-Splitting and Spin-Resolved Ballistic Transport in GaAs/AlGaAs Two-Dimensional Holes. *Phys. Rev. Lett.* **1998**, *81*, 1282−1285.

(9) Dresselhaus, G. Spin−Orbit Coupling Effects in Zinc Blende Structures. *Phys. Rev.* **1955**, *100*, 580−586.

(10) Rashba, E. I. Properties of Semiconductors with an Extremum Loop. 1. Cyclotron and Combinational Resonance in a Magnetic Field Perpendicular to the Plane of the Loop. *Sov. Phys. Solid State* **1960**, *2*, 1109. *Fiz. Tverd. Tela (Leningrad)* **1960**, *2*, 1224].

(11) *International Technology Roadmap for Semiconductors*, Executive Summary for 2009. http://www.itrs.net/links/2009ITRS/2009Chapters_2009Tables/2009_ExecSum.pdf (2009).

(12) Spintronics, P. F. Spintronics. *Nat. Mater.* **2012**, *11*, 367.

(13) Sinova, J.; Zutic, I. New Moves of the Spintronics Tango. *Nat. Mat.* **2012**, *11*, 368−371.

(14) World record for in vitro is claimed to be 80 microseconds; see: Morton, J. J. L.; Tyryshkin, A. M.; Ardavan, A.; Porfyrakis, K.; Lyon, S. A.; Briggs, G. A. D. Electron Spin Relaxation of N@C60 in CS2. *J. Chem. Phys.* **2006**, *124*, 014508.

(15) Divincenzo, D. P. Quantum Computation. *Science* **1995**, *270*, 255−261.

(16) Naber, W. J. M.; Faez, S.; van derWiel, W. G. Organic Spintronics. *J. Phys. D: Appl. Phys.* **2007**, *40*, R205−R228.

(17) Bergenti, I.; Dediu, V.; Prezioso, M.; Riminucci, A. Organic Spintronics. *Philos. Trans. R. Soc. London, Ser. A* **2011**, *369*, 3054−3068.

(18) Urdampilleta, M.; Klyatskaya, S.; Cleuziou, J.-P.; Ruben, M.; Wernsdorfer, W. Supramolecular Spin Valves. *Nat. Mater.* **2011**, *10*, 502−506.

(19) Sanvito, S. Organic Spintronics: Filtering Spins with Molecules. *Nat. Mater.* **2011**, *10*, 484−485.

(20) Thomson Kelvin, William *Baltimore Lectures on Molecular Dynamics and the Wave Theory of Light*; C.J. Clay & Sons: London, 1904. Reprinted by Cambridge University Press: Cambridge, U.K., 2010.

(21) *Comprehensive Asymmetric Catalysis*; Jacobsen, E. N., Pfaltz, A., Yamamoto, H., Eds.; Springer: Berlin, Germany, 1999. See also: (b) Yoon, T. P.; Jacobsen, E. N. Privileged Chiral Catalysts. *Science* **2003**, *299*, 1691−1693.

(22) *Catalytic Asymmetric Synthesis*, 2nd ed.; Ojima, I., Ed.; Wiley: New York, 2000.

(23) See: Yoon, T. P.; Jacobsen, E. N. Privileged Chiral Catalysts. *Science* **2003**, *299*, 1691−1693.

(24) Barron, L. D. Chirality, Magnetism and Light. *Nature* **2000**, *405*, 895−896.

(25) *Molecular Light Scattering and Optical Activity*, 2nd ed. Barron, L. D., Ed.; Cambridge University Press: Cambridge, U.K., 2004.

(26) Göhler, B.; Hamelbeck, V.; Markus, T. Z.; Kettner, M.; Hanne, G. F.; Vager, Z.; Naaman, R.; Zacharias, H. Spin Selectivity in Electron Transmission Through Self-Assembled Monolayers of dsDNA. *Science* **2011**, *331*, 894−897.

(27) Ray, K.; Ananthavel, S. P.; Waldeck, D. H.; Naaman, R. Asymmetric scattering of Polarized Electrons by Organized Organic Films Made of Chiral Molecules. *Science* **1999**, *283*, 814−816.

(28) Carmeli, I.; Skalkova, V.; Naaman, R.; Vager, Z. Magnetization of Chiral Monolayers of Polypeptide—A Possible Source of Magnetism in Some Biological Membranes. *Angew. Chem., Int. Ed.* **2002**, *41*, 761−764.

(29) Ray, S. G.; Daube, S. S.; Leitus, G.; Vager, Z.; Naaman, R. Chirality-Induced Spin-Selective Properties of Self-Assembled Monolayers of DNA on Gold. *Phys. Rev. Lett.* **2006**, *96*, 036101.

(30) Campbell, D. M.; Farago, P. S. Electron Optic Dichroism in Camphor. *J. Phys. B: At. Mol. Phys.* **1987**, *20*, 5133−5143.

(31) Nolting, C.; Mayer, S.; Kessler, J. Electron Dichroism — New Data and an Experimental Cross-Check. *J. Phys. B* **1997**, *30*, 5491−5499.

(32) Bihlmayer, G.; Blügel, S.; Chulkov, E. V. Enhanced Rashba Spin−Orbit Splitting in Bi/Ag(111) and Pb/Ag(111) Surface Alloys from First Principles. *Phys. Rev. B* **2007**, *75*, 195414.

(33) Winkler, R. *Spin−Orbit Coupling Effects in Two-Dimensional Electron and Hole Systems*; Springer Tracts in Modern Physics; Springer; New York, 2003; Vol *191*.

(34) Thomas, L. H. Motion of the Spinning Electron. *Nature* **1926**, *117*, 514.

(35) Ando, T. Spin−Orbit Interaction in Carbon Nanotubes. *J. Phys. Soc. Jpn.* **2000**, *69*, 1757−1763.

(36) De Martino, A.; Egger, R.; Hallberg, K.; Balseiro, C. A. Spin−Orbit Coupling and Electron Spin Resonance Theory for Carbon Nanotubes. *Phys. Rev. Lett.* **2002**, *88*, 206402.

(37) Huertas-Hernando, D.; Guinea, F.; Brataas, A. Spin−Orbit Coupling in Curved Graphene, Fullerenes, Nanotubes, And Nanotube Caps. *Phys. Rev. B* **2006**, *74*, 155426.

(38) Medina, E.; López, F.; Ratner, M. A; Mujica, V. Chiral Molecular Films As Electron Polarizers and Polarization Modulators. *Eur. Phys. Lett.* **2012**, DOI: arxiv.org/abs/1202.3507v1.

(39) Kuemmeth, F.; Ilani, S.; Ralph, D. C; McEuen, P. L. Coupling of Spin and Orbital Motion of Electrons in Carbon Nanotubes. *Nature* **2008**, *452*, 448−452.

(40) Gutierrez, R.; Diaz, E.; Naaman, R.; Cuniberti, G. Spin Selective Transport through Helical Molecular Systems. *Phys. Rev B* **2012**, *85*, 081404(R).

(41) Nitzan, A. Electron Transmission through Molecules and Molecular Interfaces. *Annu. Rev. Phys. Chem.* **2001**, *52*, 681−750.

(42) Guo, A.-M.; Sun, Q.-F. Spin-Selective Transport of Electron in DNA Double Helix. *Phys. Rev. Lett.* **2012**, *108*, 218102.

(43) Yeganeh, S.; Ratner, M. A; Medina, E.; Mujica, V. Chiral Electron Transport: Scattering Through Helical Potentials. *J. Chem. Phys.* **2009**, *131*, 014707.

(44) Vager, D.; Vager, Z. Spin Order without Magnetism — A New Phase of Spontaneously Broken Symmetry in Condensed Matter. *Phys. Lett. A* **2012**, *376*, 1895−1897.

(45) Naaman, R.; Sanche, L. Low Energy Electron Transmission Through Thin-Film Molecular and Biomolecular Solids. *Chem. Rev.* **2007**, *107*, 1553−1579.

(46) Kirschner, J. *Polarized Electrons at Surfaces*; Springer-Verlag: Berlin, Germany, 1985.

(47) Meier, F.; Pescia, D. Band-Structure Investigation of Gold by Spin-Polarized Photoemission. *Phys. Rev. Lett.* **1981**, *47*, 374−377.

(48) Meier, F.; Bona, G. L; Hufner, S. Experimental Determination of Exchange Constants by Spin-Polarized Photoemission. *Phys. Rev. Lett.* **1984**, *52*, 1152−1155.

(49) Borstel, G.; Wohlecke, M. Spin Polarization of Photoelectrons Emitted from Nonmagnetic Solids. *Phys. Rev. B* **1982**, *26*, 1148−1155.

(50) The percentage of polarization is defined as $S = (I_+ − I_−)/(I_+ + I_−)$, where I_+ and $I_−$ are the intensities of the signal corresponding to the spin parallel or antiparallel to the electrons' velocity, respectively.

(51) Mayer, S.; Kessler, J. Experimental Verification of Electron Optic Dichroism. *Phys. Rev. Lett.* **1995**, *74*, 4803−4806.

(52) MacLaren, D. A.; Johnston, J.; Duncan, D. A.; Marchetto, H.; Dhesi, S. S.; Gadegaarde, N.; Kadodwala, M. Asymmetric Photoelectron Transmission through Chirally-Sculpted, Polycrystalline Gold. *Phys. Chem. Chem. Phys.* **2009**, *11*, 8413−8416.

(53) Wei, J. J.; Schafmeister, C.; Bird, G.; Paul, A.; Naaman, R.; Waldeck, D. H. Molecular Chirality and Charge Transfer through Self-Assembled Scaffold Monolayers. *J. Phys. Chem. B* **2006**, *110*, 1301−1308.

(54) Xie, Z.; Markus, T. Z.; Cohen, S. R.; Vager, Z.; Gutierrez, R.; Naaman, R. Spin Specific Electron Conduction through DNA Oligomers. *Nano Lett.* **2011**, *11*, 4652−4655.

(55) Buchachenko, A. L.; Kuznetsov, D. A.; Orlova, M. A.; Markarian, A. A. Magnetic Isotope Effect of Magnesium in Phosphoglycerate Kinase Phosphorylation. *Proc. Natl. Acad. Sci. U.S.A.* **2005**, *102*, 10793−10796.

(56) Hore, P. J. Are Biochemical Reactions Affected by Weak Magnetic Fields? *Proc. Natl. Acad. Sci. U.S.A.* **2012**, *109*, 1357−1358.

(57) Guy, C. Biology and Magnetic Fields. *Contemp. Phys.* **1992**, *33*, 327−328.

(58) Ritz, T.; Adem, S.; Schulten, K. A Model for Photoreceptor-Based Magnetoreception in Birds. *Biophys. J.* **2000**, *78*, 707−718.

2186

dx.doi.org/10.1021/jz300793y | *J. Phys. Chem. Lett.* 2012, 3, 2178−2187

(59) Ritz, T.; Thalau, P.; Phillips, J. B.; Wiltschko, R.; Wiltschko, W. Resonance Effects Indicate a Radical-Pair Mechanism for Avian Magnetic Compass. *Nature* **2004**, *429*, 177.

(60) Gauger E. M.; Rieper E.; Morton J. J. L.; Benjamin S. C.; Vedral V. Sustained Quantum Coherence and Entanglement in the Avian Compass. **2011**, arXiv:0906.3725v5.

(61) Ralph, D. C.; Stiles, M. D. Spin Transfer Torques. *J. Magn. Magn. Mater.* **2008**, *320*, 1190−1216.

(62) Wang, C.; Cui, Y.-T.; Katine, J. A; Buhrman, R. A.; Ralph, D. C. Time-Resolved Detection of Spin-Transfer-Driven Ferromagnetic Resonance and Spin Torque Measurement in Magnetic Tunnel Junctions. *Nat. Phys.* **2011**, *7*, 496.

2187

dx.doi.org/10.1021/jz300793y | *J. Phys. Chem. Lett.* 2012, 3, 2178−2187